Plane Wave Diffraction by a Semi-Infinite Plate With Fractional Boundary Conditions

Takashi Nagasaka and Kazuya Kobayashi

Abstract – The problem of E-polarized plane wave diffraction by a semi-infinite plate with fractional boundary conditions is rigorously analyzed using the Wiener–Hopf technique. The Wiener–Hopf equations are solved via the factorization and decomposition procedure leading to the exact solution. The scattered field is asymptotically evaluated with the aid of the steepest descent method leading to a Fresnel integral representation. Numerical examples on the total field intensity are presented, and scattering characteristics of the semi-infinite plate are discussed.

1. Introduction

Fractional boundary conditions (FBC) [1–3] describe an intermediate case between perfect electric conductor (PEC) and perfect magnetic conductor (PMC). *Fractional* means a fractional derivative of the total electric field components in this article. The surfaces with FBC have scattering characteristics similar to the artificial magnetic conductor surfaces because the reflection phase of the surfaces with FBC is controllable by shifting the fractional order. Therefore, the analysis of the electromagnetic scattering by materials with FBC becomes a more important subject in electromagnetic theory and antenna design studies.

The diffraction problems related to FBC have been analyzed thus far in several papers. For example, [2] analyzed the plane wave diffraction problem involving a semi-infinite plate with FBC and clarified the near-field behavior. In this article, we shall consider a semi-infinite plate with FBC and rigorously analyze the E-polarized plane wave diffraction by using the Wiener–Hopf technique together with Jones's method [4–6]. Note that the Wiener–Hopf technique was applied, for the first time, in this article for the analysis of diffraction problems involving structures with FBC.

Introducing the Fourier transform of the scattered field and applying FBC in the transform domain, the problem was reduced to Wiener–Hopf equations, exactly solved via the factorization and decomposition procedure. The scattered field in the real space was evaluated by taking the Fourier inverse of the solution in the transform domain and using the steepest descent method, which led to a Fresnel integral representation. Numerical examples of the near- and far-field intensity are presented, and scattering characteristics of the semi-infinite plate are discussed. The time factor is assumed to be $\exp(-i\omega t)$ and suppressed throughout this article.

Manuscript received 27 December 2021.

Takashi Nagasaka and Kazuya Kobayashi are with the Department of Electrical, Electronic, and Communication Engineering, Chuo University, 1-13-27 Kasuga, Bunkyo-ku, Tokyo 112-8551, Japan; e-mail: nagasaka@elect.chuo-u.ac.jp, kazuya@tamacc.chuo-u.ac.jp.

2. Formulation of the Problem

We consider the diffraction of a plane wave by a semi-infinite plate with FBC as shown in Figure 1. The incident field is assumed to be of E polarization.

Let the total electric field $\phi^t(x,z)[\equiv E_y^t(x,z)]$ be

$$\phi^t(x,z) = \phi^i(x,z) + \phi(x,z) \tag{1}$$

where $\phi^i(x,z)$ is the incident field given by

$$\phi^i(x,z) = e^{-ik(x\sin\theta_0 + z\cos\theta_0)}, \quad 0 < \theta_0 < \pi/2 \tag{2}$$

In (2), $k[=\omega(\mu_0\varepsilon_0)^{1/2}]$ is the free-space wavenumber, where ε_0 and μ_0 denote the permittivity and permeability of vacuum, respectively. The term $\phi(x,z)$ in (1) is the unknown scattered field and satisfies the two-dimensional wave equation as follows:

$$\left(\partial^2/\partial x^2 + \partial^2/\partial z^2 + k^2\right)\phi(x,z) = 0 \tag{3}$$

On the surface of the semi-infinite plate, the total electric field $\phi^t(x,z)$ satisfies the FBC as given by

$$D_x^\nu E_y^t(x,z)\Big|_{x=\pm 0} = 0, \quad z < 0 \tag{4}$$

where the fractional order ν takes the value between 0 and 1, and $D_x^\nu f(x)$ denotes a fractional derivative defined by the integral of Riemann–Liouville [7, 8]

$$D_x^\nu f(x) = \frac{1}{\Gamma(1-\nu)}\frac{d}{dx}\int_{-\infty}^{x} f(t)(x-t)^{-\nu}dt \tag{5}$$

with $\Gamma(\cdot)$ being the gamma function. For $\nu = 0$, the plate with the FBC in (4) reduces to a PEC plate, and $\nu = 1$ implies a PMC plate. For intermediate values

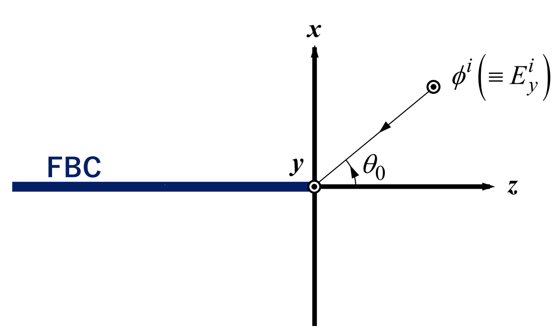

Figure 1. Geometry of the problem.

$0 < v < 1$, the FBC describes a fractional boundary with specific properties.

It is convenient to introduce a slight loss into the medium so that the free-space wavenumber k becomes complex, as in $k = k_1 + ik_2$ with $0 < k_2 \ll k_1$. It follows from the radiation condition that the asymptotic behavior of the scattered field for large $|z|$ is given by

$$\begin{aligned}\phi(x,z) &= O\left(e^{k_2 z \cos\theta_0}\right), \quad z \to -\infty \\ &= O\left(e^{-k_2 z}\right), \quad z \to \infty\end{aligned} \tag{6}$$

We define the Fourier transform of the unknown scattered field $\phi(x,z)$ with respect to z as

$$\Phi(x,\alpha) = (2\pi)^{-1/2}\int_{-\infty}^{\infty}\phi(x,z)e^{i\alpha z}dz \tag{7}$$

where $\alpha = \sigma + i\tau$. We can show from (6) and a fundamental theorem on the regularity of Fourier transforms [9] that $\Phi(x,\alpha)$ is regular in the strip $-k_2 < \tau < k_2\cos\theta_0$ of the complex α-plane. We also see that $\Phi(x,\alpha)$ is bounded for $|x| \to \infty$. If we further introduce the Fourier integrals

$$\Phi_\pm(x,\alpha) = \pm(2\pi)^{-1/2}\int_0^{\pm\infty}\phi(x,z)e^{i\alpha z}dz \tag{8}$$

we find by using theorems on the regularity of Fourier integrals [9] that $\Phi_+(x,\alpha)$ and $\Phi_-(x,\alpha)$ are regular in $\tau > -k_2$ and $\tau < k_2\cos\theta_0$, respectively. Using the notations of (8), $\Phi(x,\alpha)$ is written as

$$\Phi(x,\alpha) = \Phi_-(x,\alpha) + \Phi_+(x,\alpha) \tag{9}$$

By taking the Fourier transform of (3) and making use of the radiation condition, we find that

$$\left(d^2/dx^2 - \gamma^2\right)\Phi(x,\alpha) = 0 \tag{10}$$

for any α in the strip $-k_2 < \tau < k_2\cos\theta_0$, where $\gamma = (\alpha^2 - k^2)^{1/2}$; (10) is the transformed wave equation. Because γ is a double-valued function of α, we choose a proper branch for γ such that γ reduces to $-ik$ when $\alpha = 0$. The solution of (10), bounded for $|x| \to \infty$, is expressed as follows:

$$\begin{aligned}\Phi(x,\alpha) &= A(\alpha)e^{-\gamma x}, \quad x > 0 \\ &= B(\alpha)e^{\gamma x}, \quad x < 0\end{aligned} \tag{11}$$

where $A(\alpha)$ and $B(\alpha)$ are unknown functions. From (4) and (11), we find that

$$(-\gamma)^v A(\alpha) - \gamma^v B(\alpha) = 0 \tag{12}$$

$$(-\gamma)^v A(\alpha) + \gamma^v B(\alpha) = 2U_{(+)}(\alpha) \tag{13}$$

where

$$U_{(+)}(\alpha) = D_x^v\Phi_+(0,\alpha) - \frac{A^v}{\alpha - k\cos\theta_0} \tag{14}$$

with

$$D_x^v\Phi_+(\pm 0,\alpha) = D_x^v\Phi_+(0,\alpha) \tag{15}$$

$$A^v = -i(2\pi)^{-1/2}(-ik\sin\theta_0)^v \tag{16}$$

The parentheses in the subscript of $U_{(+)}(\alpha)$ in (14) imply that $U_{(+)}(\alpha)$ is regular in $\tau > -k_2\cos\theta_0$, except for a simple pole at $\alpha = k\cos\theta_0$.

Taking into account the boundary conditions, we obtain that

$$A(\alpha) - B(\alpha) = J_-(\alpha) \tag{17}$$

$$A(\alpha) + B(\alpha) = -J'_-(\alpha)/\gamma \tag{18}$$

where

$$J'_-(\alpha) = \frac{d}{dx}[\Phi_-(+0,\alpha) - \Phi_-(-0,\alpha)] \tag{19}$$

$$J_-(\alpha) = \Phi_-(+0,\alpha) - \Phi_-(-0,\alpha) \tag{20}$$

From (12), (13), (17), and (18), we derive, after some manipulation, that

$$U_{(+)}(\alpha) + K(\alpha)J'_-(\alpha) = 0, \quad 0 \le v < 1 \tag{21}$$

$$U_{(+)}(\alpha) + M(\alpha)J_-(\alpha) = 0, \quad 0 < v \le 1 \tag{22}$$

where

$$K(\alpha) = \frac{i^{1+v}}{e^{i\pi v} + 1}\frac{1}{(k^2 - \alpha^2)^{(1-v)/2}} \tag{23}$$

$$M(\alpha) = \frac{i^v}{e^{i\pi v} - 1}\left(k^2 - \alpha^2\right)^{v/2} \tag{24}$$

Here, (21) and (22) are the Wiener–Hopf equations satisfied by the unknown spectral functions, where $J'_-(\alpha)$ and $J_-(\alpha)$ are the Fourier transform of electric and magnetic surface currents induced on the plate, respectively. The problems for $v = 0$ and 1 correspond to the diffraction by PEC and PMC plates, respectively.

3. Exact Solution

The kernel functions $K(\alpha)$ and $M(\alpha)$ are factorized as follows:

$$K(\alpha) = K_+(\alpha)K_-(\alpha) \tag{25}$$

$$M(\alpha) = M_+(\alpha)M_-(\alpha) \tag{26}$$

where

$$K_\pm(\alpha) = \left(\frac{i^{1+v}}{e^{i\pi v} + 1}\right)^{1/2}\frac{1}{(k \pm \alpha)^{(1-v)/2}} \tag{27}$$

$$M_\pm(\alpha) = \left(\frac{i^v}{e^{i\pi v} - 1}\right)^{1/2}(k \pm \alpha)^{v/2} \tag{28}$$

Using the split functions $K_\pm(\alpha)$ and $M_\pm(\alpha)$ and applying the analytic continuation and the Liouville's theorem, we obtain from (21) and (22) that

$$J'_-(\alpha) = \frac{A^v}{K_+(k\cos\theta_0)} \frac{1}{K_-(\alpha)(\alpha - k\cos\theta_0)} \tag{29}$$

$$J_-(\alpha) = \frac{A^v}{M_+(k\cos\theta_0)} \frac{1}{M_-(\alpha)(\alpha - k\cos\theta_0)} \tag{30}$$

Thus, (29) and (30) are the exact solution of Wiener–Hopf (21) and (22), respectively.

4. Scattered Field

Taking into account the boundary conditions, the scattered field in the Fourier transform domain is expressed as

$$\Phi(x,\alpha) = \tilde{\Phi}(\alpha) e^{-\gamma|x|} \tag{31}$$

where

$$\tilde{\Phi}(\alpha) = -\frac{1}{2\gamma} J'_-(\alpha) \pm \frac{1}{2} J_-(\alpha), \quad x \gtrless 0 \tag{32}$$

Taking the inverse Fourier transform of (31), the scattered field in the real space is found to be

$$\phi(x,z) = (2\pi)^{-1/2} \int_{-\infty+ic}^{\infty+ic} \tilde{\Phi}(\alpha) e^{-\gamma|x| - i\alpha z} d\alpha \tag{33}$$

where $-k_2 < c < k_2 \cos\theta_0$.

We introduce the polar coordinate $x = \rho\sin\theta$ and $z = \rho\cos\theta$ for $-\pi < \theta < \pi$ and let $k_2 \to +0$. Using the steepest descent method [9], we can show after some manipulations that (33) is reduced to the Fresnel integral representation

$$\begin{aligned}
&\phi(\rho,\theta) \\
&\sim -h_0^{s,d}(\theta,\theta_0,v) e^{-ik\rho\cos(|\theta|+\theta_0)} F\left[(2k\rho)^{1/2}\cos\left(\tfrac{|\theta|+\theta_0}{2}\right)\right] \\
&\quad - h_0^{d,s}(\theta,\theta_0,v) e^{-ik\rho\cos(|\theta|-\theta_0)} F\left[(2k\rho)^{1/2}\cos\left(\tfrac{|\theta|-\theta_0}{2}\right)\right] \\
&\quad + H(|\theta| - \pi + \theta_0) e^{-ik\rho\cos(|\theta|+\theta_0)} \\
&\quad \cdot \left\{ h_0^{s,d}(\theta,\theta_0,v) - \frac{1}{2}\left[\left(1+e^{-i\pi v}\right) \pm \left(1 - e^{-i\pi v}\right)\right] \right\}, \\
&\quad x \gtrless 0
\end{aligned} \tag{34}$$

under the condition that $|k|\rho$ is not too small, where $F(\cdot)$ is the Fresnel integral defined by

$$F(z) = e^{-i\pi/4}\pi^{-1/2} \int_z^\infty e^{it^2} dt \tag{35}$$

and

$$\begin{aligned}
h_0^{s,d}(\theta,\theta_0,v) &= \frac{1}{2}\left(e^{-i\pi v}+1\right) \frac{\sin^v(\theta_0/2)}{\cos^v(|\theta|/2)} \\
&\quad \pm \frac{1}{2}\left(e^{-i\pi v}-1\right) \frac{\cos^{1-v}(|\theta|/2)}{\sin^{1-v}(\theta_0/2)}
\end{aligned} \tag{36}$$

$$\begin{aligned}
H(\xi) &= 1, \quad \xi > 0 \\
&= 0, \quad \xi < 0
\end{aligned} \tag{37}$$

The solution (34) reduces to exact solutions with PEC and PMC boundary conditions when $v = 0$, 1 (see the Appendix).

5. Numerical Results

We present some numerical examples of the total field intensity and discuss scattering characteristics of the semi-infinite plate. The normalized total field intensity is introduced as

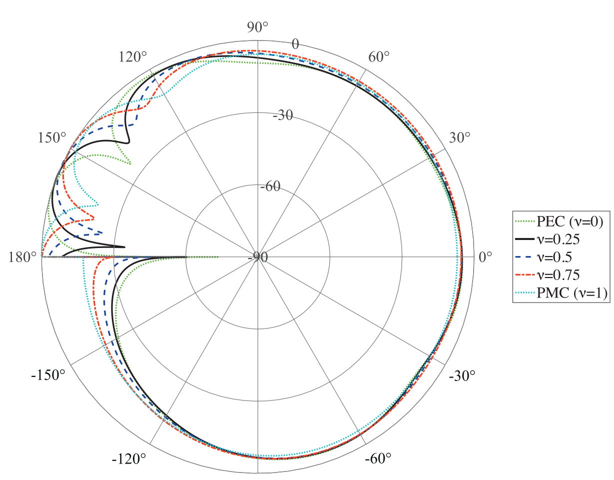

Figure 2. Total electric field $|\phi^t(\rho,\theta)|$[dB] versus observation angle θ for $\theta_0 = 60°$, $\rho = \lambda$.

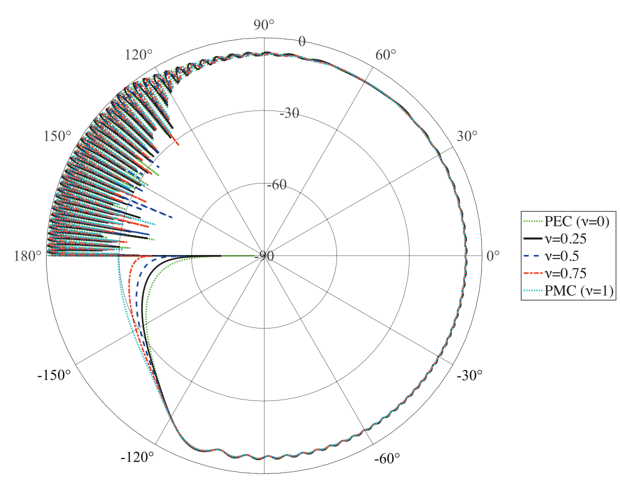

Figure 3. Total electric field $|\phi^t(\rho,\theta)|$ [dB] versus observation angle θ for $\theta_0 = 60°$, $\rho = 20\lambda$.

$$\left|\phi^t(\rho,\theta)\right|[\mathrm{dB}] = 20\log_{10}\left[\frac{\left|\phi^t(\rho,\theta)\right|}{\max\limits_{|\theta|\le\pi}\left|\phi^t(\rho,\theta)\right|}\right] \tag{38}$$

Figures 2 and 3 show numerical examples of the total field intensity as a function of observation angle θ, where the incidence angle is fixed as $\theta_0 = 60^\circ$ and the distance from the origin ρ is chosen as λ and 20λ. The fractional order v is chosen as 0 (PEC), 0.25, 0.5, 0.75, and 1 (PMC). In Figures 2 and 3, we observe by comparing the results for different v that the scattering characteristics exhibit close features within the range $-120^\circ < \theta < 90^\circ$. On the other hand, the results become very different over the ranges $-180^\circ < \theta < -120^\circ$ and $90^\circ < \theta < 180^\circ$. The differences in peak locations over $90^\circ < \theta < 180^\circ$ may be due to the phase shift of reflection by changing the value of v. Comparing the characteristics for $\rho = \lambda$ (near field) and 20λ (far field), we also see that, the total field intensity shows rapid oscillation for larger distance from the origin ρ over the range $90^\circ < \theta < 180^\circ$.

6. Conclusions

In this article, we exactly solved the plane wave diffraction by a semi-infinite plate with FBC for E polarization by using Wiener–Hopf technique. We obtained the exact solution to the Wiener–Hopf equations. The scattered field was derived with the aid of the steepest descent method, leading to a Fresnel integral representation. We carried out numerical computation of the normalized field intensity and investigated the scattering characteristics of the semi-infinite plate with FBC.

7. References

1. E. I. Veliev, M. V. Ivakhnychenko, and T. M. Ahmedov, "Fractional Boundary Conditions in Plane Wave Diffraction on a Strip," *Progress in Electromagnetics Research*, **79**, January 2008, pp. 443-462.
2. E. Veliyev, V. Tabatadze, K. Karaçuha, and E. Karaçuha, "The Diffraction by the Half-Plane With the Fractional Boundary Condition," *Progress in Electromagnetics Research M*, **88**, January 2020, pp. 101–110.
3. V. Tabatadze, K. Karaçuha, E. Veliev, and E. Karaçuha, "Diffraction of the Electromagnetic Plane Waves by Double Half-Plane with Fractional Boundary Conditions," *Progress in Electromagnetics Research M*, **101**, March 2021, pp. 207–218.
4. D. S. Jones, "A Simplifying Technique in the Solution of a Class of Diffraction Problems," *Quarterly Journal of Mathematics*, **3**, 1, January 1952, pp. 189-196.
5. B. Noble, *Methods Based on the Wiener-Hopf Technique for the Solution of Partial Differential Equations*, London, Pergamon, 1958.
6. R. Mittra and S. W. Lee, *Analytical Techniques in the Theory of Guided Wave*, New York, Macmillan Company, 1971.
7. N. Engheta, "Use of Fractional Integration to Propose Some Fractional Solutions for the Scalar Helmholtz Equation," *Progress in Electromagnetics Research*, **12**, January 1996, pp. 107-132.
8. S. G. Samko, A. A. Kilbas, and O. I. Marichev, *Fractional Integrals and Derivatives: Theory and Applications*, Langhorne, PA, Gordon and Breach Science Publishers, 1993.
9. K. Kobayashi, "Wiener-Hopf and Modified Residue Calculus Techniques," in E. Yamashita (ed.), *Analysis Methods for Electromagnetic Wave Problems*, Boston, Artech House, 1990, Chapter 8.

Appendix. Exact Solutions for Semi-Infinite PEC and PMC Plates

This appendix is concerned with exact solutions to the diffraction problems involving PEC ($v = 0$) and PMC ($v = 1$) plates. Substituting $v = 0$, 1 into (33) and using (16) and (27)–(32), we obtain

$$\phi(x,z)\big|_{v=0} = -\frac{1}{2\pi i}\int_{-\infty+ic}^{\infty+ic}\frac{(2k)^{1/2}\cos\frac{\theta_0}{2}e^{-\gamma|x|-i\alpha z}}{(k+\alpha)^{1/2}(\alpha-k\cos\theta_0)}d\alpha \tag{A1}$$

$$\phi(x,z)\big|_{v=1} = \pm\frac{1}{2\pi i}\int_{-\infty+ic}^{\infty+ic}\frac{(2k)^{1/2}\sin\frac{\theta_0}{2}e^{-\gamma|x|-i\alpha z}}{(k-\alpha)^{1/2}(\alpha-k\cos\theta_0)}d\alpha \tag{A2}$$

for $x \gtrless 0$, respectively. A closed form evaluation of (A1) in terms of the Fresnel integral is discussed in detail in [9]. Following a procedure similar to that used in [9], we can reduce (A2) to the Fresnel integral representation. Thus, we arrive at the following result:

$$\begin{aligned}\phi(\rho,\theta)\big|_{v=0,1} = &-e^{-ik\rho\cos(\theta-\theta_0)}F\left[(2k\rho)^{1/2}\cos\frac{\theta-\theta_0}{2}\right]\\ &\mp e^{-ik\rho\cos(\theta+\theta_0)}F\left[(2k\rho)^{1/2}\cos\frac{\theta+\theta_0}{2}\right]\end{aligned} \tag{A3}$$